Available online at www.sciencedirect.com
SCIENCE DIRECT
Journal of Power Sources 156 (2006) 634–644
JOURNAL OF POWER SOURCES
www.elsevier.com/locate/jpowsour

Is 3-methyl-2-oxazolidinone a suitable solvent for lithium-ion batteries?

L. Gzara [a], A. Chagnes [b], B. Carré [b], M. Dhahbi [a], D. Lemordant [b,*]

[a] *Laboratoire Eau et Technologies Membranaires, INRST, BP 95 Hammam-Lif 2050, Tunisia*
[b] *Laboratoire de Chimie-Physique des Interfaces et des Milieux Electrolytiques (EA2098), Université F. Rabelais, Parc de Grandmont, 37200 Tours, France*

Received 2 December 2004; received in revised form 24 June 2005; accepted 27 June 2005
Available online 31 August 2005

Abstract

3-Methyl-2-oxazolidinone (MeOx) has been mixed to ethylene carbonate (EC) or dimethyl carbonate (DMC) in presence of lithium tetrafluoroborate ($LiBF_4$) or lithium hexafluorophosphate ($LiPF_6$) for use as electrolyte in lithium batteries. The optimized electrolytes in term of conductivity and viscosity are MeOx:EC, x(MeOx) = 0.5 and MeOx:DMC, x(MeOx) = 0.4 in presence of $LiBF_4$ (1 M) or $LiPF_6$ (1 M). MeOx:EC electrolytes have a better thermal stability than MeOx:DMC electrolytes but the low wettability of the Celgard separator by MeOx:EC prevents its use in lithium batteries. No lithium insertion–deinsertion occurs when $LiPF_6$ is used as salt in MeOx-based electrolytes. MeOx:DMC, x(MeOx) = 0.4 + $LiBF_4$ (1 M) exhibits a good cycling ability at a graphite electrode but all the investigated electrolytes containing MeOx have a low stability in oxidation at a lithium cobalt oxide electrode (Li_xCoO_2).

Keywords: Electrolyte; 3-Methyl-2-oxazolidinone; Lithium battery; Conductivity; DSC

1. Introduction

The search for new electrolytes in lithium-ion batteries has intensified in recent years but electrolytes composed of ethylene carbonate (EC), diethyl carbonate (DEC), dimethyl carbonate (DMC) or propylene carbonate (PC) in presence of lithium hexafluorophosphate ($LiPF_6$) are still the reference electrolytes in the field of lithium batteries. For practical use in lithium batteries, the electrolyte has to conform to several properties such as a low viscosity to enhance the ion mobility, a high conductivity to decrease the ohmic resistance in the battery, a high dielectric constant to permit the dissociation of the lithium salt. Propylene carbonate is an interesting solvent for its physical properties but it was pointed as responsible in the exfoliation of crystalline carbons, whereas ethylene carbonate (EC) or other carbonates would prevent it [1,2] though the difference of behavior of such close molecules is not yet fully understood.

2-Oxazolidinones are heterocyclic compounds known synonymously as cyclic carbamates or cyclic urethans. Most 2-oxazolidinones are solids under normal conditions but several simple *N*-alkyl-substituted derivatives, like 3-methyl-2-oxazolidinone (MeOx), are usually liquid at room temperature [3]. MeOx may be an alternative co-solvent in electrolytes for lithium batteries because this organic solvent has a high dielectric constant (Table 1).

In order to preserve the high dielectric constant of MeOx while forming onto the graphite electrode a high quality passivative film, physicochemical and electrochemical properties of a binary mixture of MeOx and EC have been investigated in presence of lithium salts such as lithium hexafluorophosphate or lithium tetrafluoroborate. As this electrolyte is viscous, a mixture of MeOx with DMC in presence of lithium hexafluorophosphate has also been studied to enhance the ion mobility. This addition of DMC to MeOx enhances the wettability of the Celgard separator by lowering the superficial tension and permits a better penetration of the electrolyte into the pores of the separator. The thermal stability of MeOx:EC and MeOx:DMC mixtures versus the co-solvent composition

* Corresponding author. Tel.: +33 2 47366953; fax: +33 2 47367073.
E-mail address: daniel.lemordant@univ-tours.fr (D. Lemordant).

0378-7753/$ – see front matter © 2005 Elsevier B.V. All rights reserved.
doi:10.1016/j.jpowsour.2005.06.032

Table 1
Physicochemical properties of EC, DMC and MeOx

	ε_r	μ (D)	η (cP)	ρ (g cm^{-3})	T_m (°C)	T_b (°C)
EC	89[a]	4.80[b]	1.9[c]	1.321[d]	35–37[e]	238 at 760 mmHg[b]
DMC	3.12[b]	0.75[f]	0.585[b]	1.069[d]	4[b]	90 at 760 mmHg[b]
MeOx	77.5[g]	5.00[h]	2.45[g]	1.044[g]	15[g]	87–90 at 1 mmHg[h]

ε_r: Dielectric constant (25 °C); μ: dipolar moment; η: viscosity (25 °C for DMC and MeOx; 40 °C for EC); ρ: density (25 °C); T_m: melting temperature; T_b: boiling temperature.
[a] Ref. [4].
[b] Ref. [5].
[c] Ref. [6].
[d] Ref. [7].
[e] Ref. [8].
[f] From Alchemy calculation (PM3 semi-empirical method).
[g] Ref. [9].
[h] Ref. [10].

in presence or in absence of lithium salt has been investigated because the search of new electrolytes with a high thermal stability is of great importance [11–21]. Conductivity measurements versus salt concentration, co-solvent composition and temperature have been carried out to optimize the composition of MeOx:EC and MeOx:DMC electrolytes. Activation energy for the conductivity has been calculated to evaluate the temperature dependence of the conductivity. The oxidation and reduction properties of the optimized electrolytes have also been investigated as well as the cycling ability at graphite and Li_xCoO_2 electrodes.

2. Experimental

3-Methyl-2-oxazolidinone (MeOx), ethylene carbonate (EC) and dimethyl carbonate (DMC) (purity > 99%) were purchased from Aldrich, dried over molecular sieves prior to use and stored under argon atmosphere. $LiPF_6$ (99.99%) and $LiBF_4$ (99.99%) were obtained from Fluka and used as received. The water content of the solutions was lower than 50 ppm as indicated by Karl Fisher titration. A dry box filled with argon is used for the preparation of all solutions studied here.

In order to optimize the composition of the electrolytes, ac conductivity measurements were carried out using a Crison GLP 31 and a Crison S2-92 conductivity cell equipped with platinum electrodes (cell constant = 1 cm^{-1}). All the compositions of the mixtures are reported in molar fraction of MeOx (quoted x(MeOx)).

Viscosity measurements were obtained using an Ubbelhode capillary immersed in a thermostated bath (±0.02 °C) and a Schott (AUS 310) viscometer. Densities were determined using a vibrating tube densimeter (Picker).

A DSC 6 Perkin-Elmer Differential Scanning Calorimeter (DSC) was used for DSC experiments. Thermograms were carried out at 10 K min^{-1} from 25 to 390 °C in 50 μL aluminum pans containing a small volume of electrolyte (10–20 μL). The pans were not hermetically sealed but the cover was holed to permit the evacuation of the gas produced by the thermal decomposition of the electrolyte. The reference cell was an aluminum pan filled with silica powder.

The graphite and Li_xCoO_2 electrodes were kindly provided by SAFT (Bordeaux). The graphite electrode is composed of a mixture of artificial graphites with a practical capacity of 280 mAh g^{-1}. Graphite and Li_xCoO_2 electrodes were dried under reduced pressure at 150 °C during 8 h prior to use. Celgard® 2000 membrane was dried at 60 °C during 24 h under room pressure.

The electrochemical experiments were run using a VersaStat™ (EG & G Instruments) potentiostat for linear sweep and cyclic voltammetry on a rotating platinum electrode. An Arbin electrochemical device equipment was used for linear sweep voltammetries, cyclic voltammetries and cycling ability tests at a graphite and a Li_xCoO_2 electrodes.

3. Results and discussion

3.1. Thermal behavior of the MeOx mixtures

3.1.1. MeOx:EC mixtures

The DSC thermograms of MeOx:EC mixtures in absence of lithium salt are reported in Fig. 1a. For x(MeOx) = 0, the first endothermic peak at 35 °C corresponds to the fusion of EC and the second one at 240 °C is attributed to the vaporization of EC. These temperatures are in agreement with the melting and boiling temperatures reported in the literature (Table 1). For x(MeOx) = 1 (Fig. 1a), the thermogram exhibits an endothermic peak attributed to the vaporization of MeOx at 259 °C. For x(MeOx) = 0.3 and x(MeOx) = 0.8, the first and second endothermic peaks are respectively attributed to the vaporization of the corresponding MeOx:EC mixture and pure solvents (EC or MeOx). For x(MeOx) = 0.5, the mixture corresponds to the azeotropic composition as only one peak is observed at 110 °C (onset of the peak). The low azeotropic composition evidences a destructuring of EC induced by the presence of MeOx.

The influence of the addition of $LiBF_4$ (1 M) or $LiPF_6$ (1 M) on the thermal stability of the mixtures are displayed

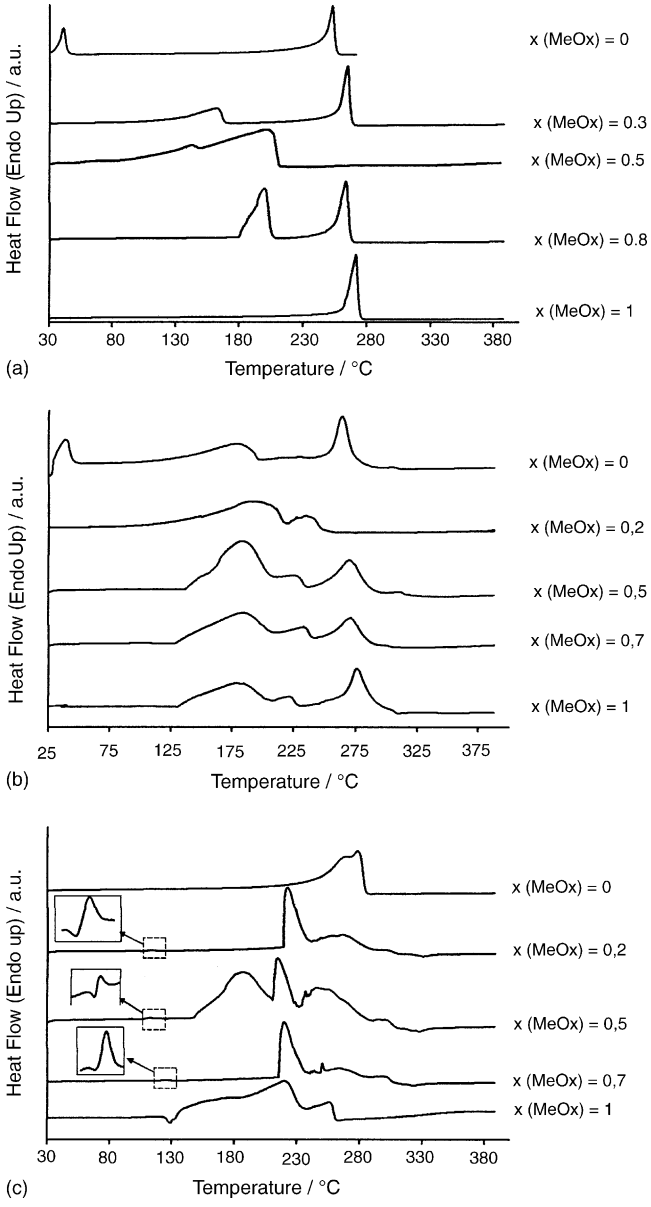

Fig. 1. DSC thermograms of MeOx:EC mixtures at 10 K min^{-1}: (a) in absence of lithium salt; (b) in presence of $LiBF_4$ (1 M); (c) in presence of $LiPF_6$ (1 M) (x(MeOx) relative to the weight fraction of MeOx in the mixture).

respectively in Fig. 1b and c. In presence of $LiPF_6$, it can be noticed that EC remains liquid at room temperature whereas EC is solid in presence of $LiBF_4$ and consequently the first endothermic peak at 28 °C corresponds to the fusion of EC (Fig. 1b). The two other endothermic peaks at 129 and 248 °C are respectively attributed to the vaporization of EC molecules which interact with lithium salt and free molecules of EC. EC and MeOx interact strongly with each other due to their high dipole moments (Table 1) [22,23] and the addition of lithium salts in a mixture of EC and MeOx involves a destructing of the mixture. The same behavior is observed when $LiPF_6$ is added to EC (Fig. 1c). The destructuring of the solvent seems to be more important in presence of $LiBF_4$ than with $LiPF_6$. Fig. 1b shows that the thermogram exhibits only two endothermic peaks at 150 °C and 225 °C for x(MeOx) = 0.2 and three endothermic peaks are observed above 125 °C for the MeOx rich region (x(MeOx) ≥ 0.5). The first peak appears at 125 °C for x(MeOx) ≥ 0.5. The end of the second peak is observed at 228 °C for x(MeOx) = 0.5, 234 °C for x(MeOx) = 0.7 and 223 °C for x(MeOx)=1. The onset of the last peak begin at 241, 245 and 247 °C for x(MeOx) = 0.5, 0.7 and 1, respectively. The first peak may be attributed to the vaporization of solvating molecules of EC, the second one may be attributed to the vaporization of solvating MeOx molecules and the last peak may correspond to the vaporization of free MeOx and free EC molecules in accordance with the values reported in Table 1. For all DSC thermograms, no decomposition of $LiBF_4$ occurs between 25 and 390 °C.

The thermal stability of MeOx–EC mixtures in presence of $LiPF_6$ has been investigated and the DSC thermograms are displayed in Fig. 1c. For x(MeOx) = 0.2 and 0.5, an endothermic peak at 107 °C is followed by an exothermic peak at 114 °C (Fig. 1c). These peaks are attributed to the presence of $LiPF_6$ in the mixture as they are not observed in absence of lithium salt or in presence of $LiBF_4$. For x(MeOx) = 0.7, these peaks are shifted to higher temperatures (119 and 125 °C). MeOx + $LiPF_6$ exhibits only one exothermic peak at 130 °C which may be attributed to the decomposition of $LiPF_6$ involving the formation of PF_5 (gas) and LiF [24,25]. PF_5 may react with the trace of water to form HF and POF_3 [26–28].

For x(MeOx) = 0.2, 0.5 and 0.7, the endothermic peak may be attributed to the decomposition of $LiPF_6$ and the exothermic peak may be attributed to an hydrolysis of EC by HF [29] as no similar peaks are observed in this range of temperature in MeOx:DMC + $LiPF_6$ (Fig. 2c) or in MeOx:EC + $LiBF_4$ electrolytes (Fig. 1b).

In Fig. 1c, for x(MeOx) = 0.2 and x(MeOx) = 0.7, two endothermic peaks are observed at 219 and 265 °C whereas for x(MeOx) = 0.5, the thermogram exhibits an endothermic peak at 150 °C, and two broad peaks at 215 and 250 °C. For x(MeOx) = 1, two endothermic peaks are observed at 179 and 235 °C.

DSC thermograms show that the addition of MeOx in EC or lithium salt in MeOx:EC mixtures decreases the thermal stability. All the mixtures (in presence or in absence of lithium salts) have a thermal stability lower than 129 °C but higher than the thermal stability of the electrolyte EC:DEC:DMC (2:2:1) + $LiPF_6$ (1 M) usually used as a standard for lithium-ions batteries [30].

3.1.2. MeOx:DMC mixtures

In Fig. 2a, DSC thermograms of MeOx:DMC mixtures in absence of lithium salt are displayed. For x(MeOx) = 0.2, the presence of two endothermic peaks located at 84 and 140 °C attributed respectively to the vaporization of DMC and MeOx shows that MeOx interacts strongly with DMC. The presence of DMC involves the destructuration of the MeOx molecules and consequently decreases the temperature of vaporization

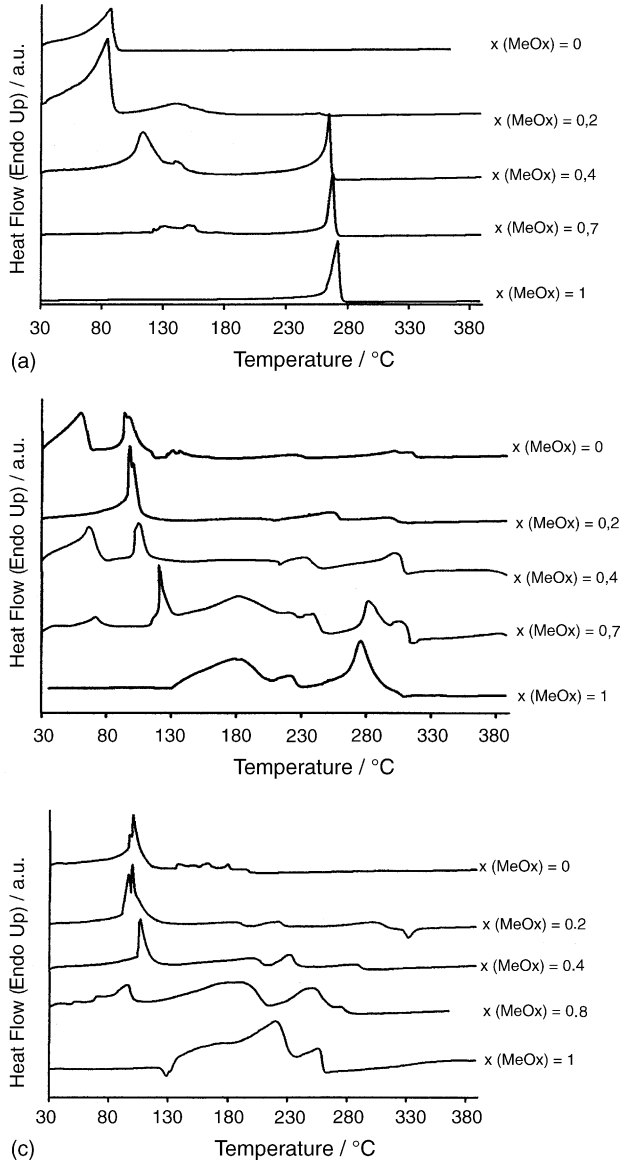

Fig. 2. DSC thermograms at 10 K min^{-1} of MeOx:DMC mixtures: (a) in absence of lithium salt: (b) in presence of $LiBF_4$ (1 M); (c) in presence of $LiPF_6$ (1 M) (x(MeOx) relative to the weight fraction of MeOx in the mixture).

of MeOx. For x(MeOx) = 0.4 and 0.7, a new endothermic peak is located at 265 °C. It may be attributed to the vaporization of MeOx which does not interact with DMC.

DSC thermograms of MeOx:DMC mixtures in presence of $LiBF_4$ (1 M) are gathered in Fig. 2b. For x(MeOx) = 0, the two endothermic peaks at 61 and 92 °C are respectively attributed to molecules of DMC in interaction with the salt and free molecules of DMC. Other endothermic peaks are observed when MeOx is added to DMC and may be attributed to MeOx molecules in interaction with $LiBF_4$, free MeOx molecules and MeOx molecules which interact with DMC molecules. Nevertheless, it is impossible to identify clearly each peak of the thermograms due to the presence of numerous solvates. Similar thermograms are obtained when $LiPF_6$ is added

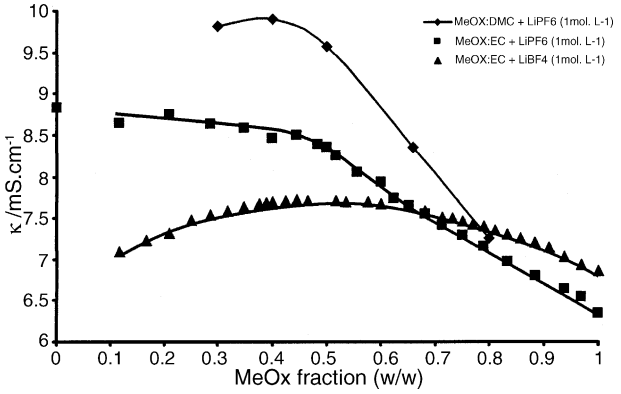

Fig. 3. Conductivity of $LiBF_4$ (1 M) and $LiPF_6$ (1 M) in MeOx:EC and MeOx:DMC mixtures vs. the weight fraction in MeOx quoted x(MeOx) at 25 °C.

to MeOx:DMC mixtures (Fig. 2c). From these results, it is obvious that MeOx:DMC + $LiPF_6$ and MeOx:DMC + $LiBF_4$ electrolytes have similar thermal stability.

The thermal stability of these electrolytes does not play an important role for the optimization of the formulation as DSC experiments shows that the thermal behavior of the investigated MeOx-based electrolytes are similar.

3.2. Formulation of the optimized electrolyte

Conductivity is one of the important factors to take into account for the formulation of an electrolyte for electrochemical systems. The influence of the weight fraction of MeOx, the temperature and the salt concentration ($LiBF_4$ and $LiPF_6$) on the conductivity in MeOx:EC and MeOx:DMC mixtures have been studied in order to optimize the composition of the electrolytes for its use in lithium batteries.

3.2.1. Effect of the mixture composition on the conductivity

Conductivities at room temperature of $LiBF_4$ (1 M) and $LiPF_6$ (1 M) in MeOx-based electrolytes (MeOx:EC and MeOx:DMC) versus the weight fraction of MeOx are displayed in Fig. 3. The conductivity of MeOx:DMC + $LiPF_6$ (1 M) electrolytes is better than the conductivity of MeOx:EC + $LiPF_6$ (1 M) because DMC decreases strongly the viscosity of the mixtures owing to its low viscosity (Table 1).

The addition of EC in MeOx in presence of $LiBF_4$ does not alter significantly the ionic conductivity (Fig. 3) and the viscosity (Table 2) as the conductivity varies between 7 and 7.7 mS cm^{-1} for $0.1 \leq x(\text{MeOx}) \leq 1$ and the viscosity is equal

Table 2
Viscosity in MeOx:EC electrolytes at 25 °C

	MeOx			MeOx:EC x(MeOx) = 0.5		
	Without salt	$LiPF_6$ (1 M)	$LiBF_4$ (1 M)	Without salt	$LiPF_6$ (1 M)	$LiBF_4$ (1 M)
η (cP)	2.48	8.35	6.87	2.68	6.88	6.50

to 6.87 cP for MeOx + $LiBF_4$ (1 M) and 6.50 cP for MeOx:EC with x(MeOx) = 0.5 in presence of $LiBF_4$ (1 M).

The addition of $LiPF_6$ in MeOx involves a more important increase in viscosity than the addition of $LiBF_4$ owing to the strong interaction between PF_6^- and MeOx (Table 2). For x(MeOx) ≤ 0.65 the conductivity of $LiPF_6$-based electrolyte is higher than the conductivity of $LiBF_4$-based electrolyte. For this range of weight fraction in MeOx, the difference of conductivity may be explained by a weak interaction between PF_6^- and EC molecules which are in majority in the EC-rich region. For the MeOx-rich region, ion–solvent interactions may be mainly attributed to ion–MeOx interactions due to the low amount of EC in these mixtures. For this range of weight fractions, the conductivity of $LiPF_6$-based electrolyte is lower than the conductivity of $LiBF_4$-based electrolyte due to the MeOx–PF_6^- interactions which are stronger than the MeOx–BF_4^- interactions as evidenced by viscosity measurements.

From conductivity and viscosity measurements, it can be concluded that the optimized MeOx-based electrolytes are MeOx:DMC with x(MeOx) = 0.5 in presence of $LiPF_6$ and MeOx:EC with x(MeOx) = 0.4 in presence of $LiPF_6$.

3.2.2. Effect of the temperature on the conductivity

In the case of the conductance, the driving force acting on the moving ions is the electrical force due to the applied electrical field and the molar conductance Λ (=κ/C) given by the theory is [31]:

$$\Lambda = \left(\frac{FL^2 z_+ z_- e}{h}\right) \exp\left(\frac{\Delta S_\Lambda^\#}{R}\right) \exp\left(\frac{-\Delta H_\Lambda^\#}{RT}\right) \quad (1)$$

where F is the faraday constant, z_+ and z_- the valency of the ions, L the mean jump distance for the ions, $\Delta S_\Lambda^\#$ and $\Delta H_\Lambda^\#$ the entropy and the enthalpy of activation for the conductivity. In a limited range of temperature, where $\Delta S_\Lambda^\#$ is independent of the temperature, the variations of the molar conductivity of a liquid electrolyte with temperature are well described by the appropriate Arrhenius-type expression:

$$\Lambda = A_\Lambda \exp\left(\frac{-E_{a,\Lambda}}{RT}\right) \quad (2)$$

where $E_{a,\Lambda}$ is the activation energy for the ionic transport by migration and A_Λ the corresponding pre-exponential term. Plots of ln(Λ) versus 1/T are linear for all the mixtures under study. $E_{a,\Lambda}$ values have been deduced from the slopes of the lines. Fig. 4 shows the variations of the activation energy ($E_{a,\Lambda}$), in the MeOx:EC and MeOx:DMC mixtures in presence of $LiPF_6$. It shows that $E_{a,\Lambda}$ is approximately independent on the MeOx:EC proportions and have a mean value of 17.39 kJ mol^{-1} (σ = 0,48) whereas $E_{a,\Lambda}$ is strongly dependent of x(MeOx) in the MeOx:DMC mixtures.

3.2.3. Effect of the salt concentration on the conductivity

For diluted electrolyte solutions the variations in Λ are described by the classical Debye–Hükel–Onsager (DHO) equation [32]: $\Lambda = \Lambda^\circ - SC^{1/2}$, where Λ° is the molar conductivity at infinite dilution and S a calculable parameter which depends on both the physical properties of the solvent and the nature of the electrolyte. Experimental results indicate that the DHO equation is not followed, except at very low concentration (C < 0.001 M) and, even in these conditions, the experimental slope (S_{exp}) is often different from the calculated one (S_{calc}) [33]. Attempts to correct experimental results for ion association are not successful and the discrepancies between theory and experience remain [34]. Clearly, in concentrated organic electrolytes, the conductivity process is different from the model embodied in the DHO equation. Another approach has been provided by the use of the quasi-lattice theory [35,36]. This theory, initially introduced to relate the mean ionic activity coefficient of electrolytes to the variation in salt concentration, has been adapted for conductivity studies [37]. In the framework of this theory, the Debye length κ_D in the ionic cloud model is replaced, at high ionic strength, by κ_L the average distance between ions of opposite charge, supposed to be distributed on the vertices of an expanded lattice [38]:

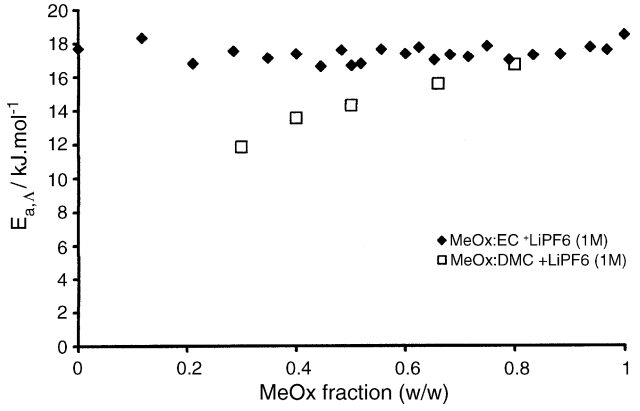

Fig. 4. Activation energy for the conductivity vs. the weight fraction in MeOx (quoted x(MeOx)) of the optimized electrolytes containing MeOx:EC and MeOx:DMC mixtures in presence of $LiPF_6$ (1 M).

$$\kappa_L = M(2000 N_a C)^{1/3} \quad (3)$$

M is the lattice parameter (equivalent to a Madelung constant), N_a the Avogadro's number and C, in mol L^{-1}, the salt concentration. According to this theory, the variations of Λ with C are described by the following set of equation:

$$\Lambda = \Lambda^{\circ\prime} - S'C^{1/3} \quad (4)$$

where

$$S' = S_1 + S_2\Lambda^{\circ\prime} \quad (5)$$

$$S_1 = \frac{0.293e^2}{\{(4\pi\varepsilon_0\varepsilon_r k_b T)M(2N_a)^{1/3}\}} \quad (6)$$

$$S_2 = \frac{N_a e^2}{\{(\pi\eta)M(2N_a)^{1/3}\}} \quad (7)$$

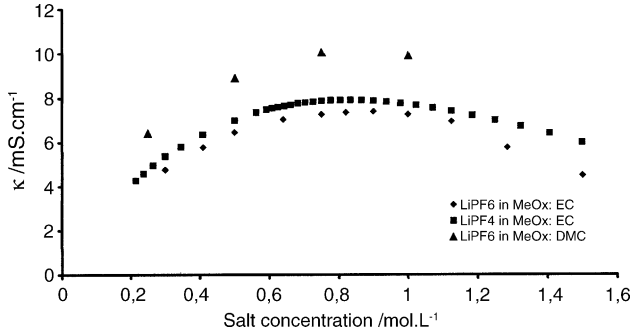

Fig. 5. Conductivity vs. the salt concentration at 25 °C of the optimized electrolytes containing $LiBF_4$ (1 M) and $LiPF_6$ (1 M) in MeOx:EC and $LiPF_6$ (1 M) in MeOx:DMC mixtures.

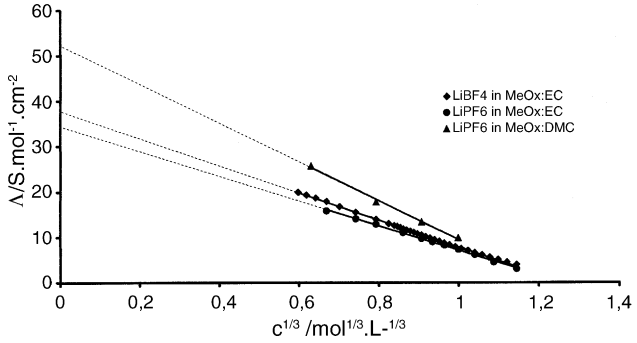

Fig. 6. Variation of the molar conductivity at 25 °C of $LiBF_4$ (1 M) and $LiPF_6$ (1 M) in MeOx:EC and $LiPF_6$ (1 M) in MeOx:DMC mixtures versus the cube root of the salt concentration.

where ε_0 is the permittivity of free space, ε_r the relative permittivity of the solvent, e the electronic charge, k_b the Boltzmann's constant, T the temperature, $\Lambda^{\circ\prime}$ (in S cm^{-1}) is the molar conductivity of the salt at infinite dilution given by the lattice model.

The quasi-lattice theory was recently verified successfully in an aprotic dipolar organic solvent (γ-butyrolactone) in presence of lithium salts such as lithium hexafluorophosphate, lithium tetrafluoroborate, lithium perchlorate and lithium hexafluorophosphate [39–41].

A high concentration in salt is required for the electrolytes used in batteries to avoid polarisation at the electrode/electrolyte interface. Therefore, it was considered a range of concentration spreading from 0.2 to 1.5 M in the solvents mixtures. The curves plotted in Fig. 5 represent the variation of the conductivity (κ) of $LiPF_6$ (1 M) and $LiBF_4$ (1 M) in MeOx:EC x(MeOx) = 0.5 and MeOx:DMC x(MeOx) = 0.4 mixtures versus the salt concentration at 25 °C. A maximum of conductivity is obtained around 0.9 mol L^{-1} for all electrolytes studied here. At this concentration, the conductivity of $LiPF_6$ in MeOx:DMC solution (10.0 mS cm^{-1}) is greater than those of $LiPF_6$ or $LiBF_4$ in MeOx:EC (respectively 7.4 and 7.9 mS cm^{-1}). For higher salt concentration, a decrease of the conductivity is observed due to the increase of the bulk viscosity involving a decrease of the ionic mobility of the ions. Another reason for the decrease of the conductivity at high electrolyte salt concentrations is increasing ion association but it was noticed that, generally, the dissociation coefficient in organic dipolar aprotic solvents such as γ-butyrolactone or valerolactone remains constant when salt is added even at high salt concentration [42,43].

In Fig. 6, the variations of Λ for $LiPF_6$ in the optimized electrolytes have been plotted against the cube root of the salt concentration. As expected from Eq. (2), linear plots are obtained for all electrolytes under consideration.

The maximum of conductivity value (C_{max}) is easily deduced from Eq. (2) by derivation of κ relatively to the concentration [39,40]:

$$C_{max} = \left(\frac{3\Lambda^{\circ\prime}}{4S'}\right)^3 \quad (8)$$

$\Lambda^{\circ\prime}$ is the molar conductivity at infinite dilution and (S') is the slope of the linear function $\Lambda = f(C^{1/3})$ which can be calculated by using Eqs. (5)–(7).

In Table 3 are reported the slopes (S'), ordinates ($\Lambda^{\circ\prime}$) and the salt concentration at maximum of conductivity obtained from experimental data and values calculated by Eq. (8). As expected, the calculated concentrations (C_{max}) are in agreement with the calculated values.

Conductivity, viscosity and thermal stability investigations of MeOx-based electrolytes in presence of lithium salts shows MeOx–EC with x(MeOx) = 0.5 and MeOx:DMC with x(MeOx) = 0.4 in presence of $LiPF_6$ or $LiBF_4$ at a concentration of 1 M may be relevant electrolytes for lithium batteries application. In the following part of this paper, electrochemical properties at platinum, graphite and Li_xCoO_2 electrodes have been investigated in these optimized electrolytes.

3.3. Electrochemical behavior

3.3.1. Electrochemical windows at a platinum electrode

The electrochemical windows of $LiPF_6$ and $LiBF_4$-based electrolytes in MeOx:EC (x(MeOx) = 0.5) and MeOx:DMC (x(MeOx) = 0.4) have been studied at a platinum rotating disc electrode for a rotating speed of 1000 rpm (scan rate = 5 mV s^{-1}). In Fig. 7a, is displayed the voltammograms of MeOx:EC and MeOx:DMC electrolytes at a platinum electrode. At a current density of 100 μA cm^{-2}, the oxidation potential of the electrolyte are: 4.5 V for MeOx:DMC + $LiBF_4$, 4.3 V for MeOx:DMC + $LiPF_6$, 4.6 V for MeOx:EC + $LiBF_4$ and MeOx:EC+$LiPF_6$. At a current density of 10 μA cm^{-2}, the oxidation potential of theses

Table 3
Ordinates ($\Lambda^{\circ\prime}$) and slopes (S') in the correlation $\Lambda = f(C^{1/3})$ and salt concentration at the maximum of conductivity

Electrolyte	$\Lambda^{\circ\prime}$	S'	C_{max}	C_{max} (given by Eq. (8))
$LiPF_6$ in MeOx:DMC	52.26	42.68	0.85	0.77
$LiPF_6$ in MeOx:EC	34.38	27.24	0.91	0.85
$LiBF_4$ in MeOx:EC	37.71	29.86	0.87	0.85

C_{max} in mol L^{-1} at 25 °C.

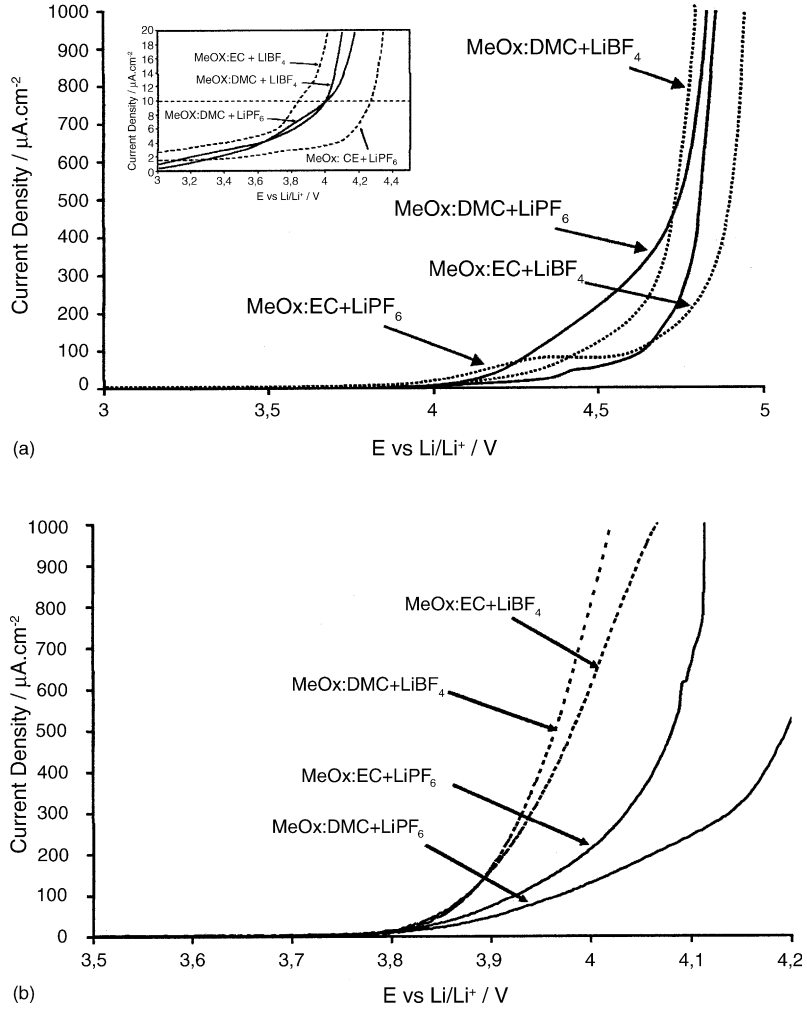

Fig. 7. Electrochemical window at (a): a Pt electrode for a rotating speed of 1000 rpm and a scan rate of 5 mV s^{-1} for MeOx-based electrolytes; (b) a $LiCoO_2$ electrode without convection and at a at scan rate of 0.5 mV s^{-1} for MeOx-based electrolytes.

electrolytes is equal to 3.8 V for MeOx:EC + $LiBF_4$, 4.2 V for MeOx:EC + $LiPF_6$, and 4 V for MeOx:DMC based-electrolytes. As these potentials correspond already to an important decomposition of the electrolyte, it is inferred that high potential cathodes will not be suitable for electrolytes containing MeOx. Moreover, if a high potential cathode material is used instead of platinum, the oxidation potential may be lowered (depleted) (refer to paragraph 3.3.2).

3.3.2. Electrochemical behavior at a Li_xCoO_2 electrode

Linear sweep voltamogramms at a Li_xCoO_2 electrode are usually characterized by three successive oxidation peaks. The first peak at 3.9 V is associated to the de-intercalation of lithium ions according to [45]:

$$Li_xCoO_2 \rightarrow Li_{1-x}CoO_2 + xLi^+ + xe^-$$

and the two following peaks, between 4.2 and 4.8 V, are attributed to phase transition occurring in the electrode material.

Linear sweep voltammetries have been performed at a Li_xCoO_2 composite electrode at a scan rate of 0.5 mV s^{-1} (Fig. 7b). The oxidation potential for a current density of 10 µA cm^{-2} is 3.8 V for all the investigated electrolytic mixtures. No lithium de-insertion occurs due to the oxidation of the electrolyte at potential lower than the de-intercalation mentioned previously (4.2 V). The electrochemical window of an electrolyte depends on the composition of the electrolyte and the nature of the electrode material. In fact, the oxidation potentials at a current density of 10 µA cm^{-2} of the MeOx based electrolytes is equal to 4 V when a platinum electrode is used instead of Li_xCoO_2 and the oxidation potential is 3.8 V when Li_xCoO_2 is used as working electrode. The difference of oxidation potential may be explained by a catalytic effect of the Li_xCoO_2 surface which favorizes the oxidation of the MeOx based electrolytes. Consequently, charging–discharging cycles are impossible. In order to obtain charging–discharging cycles, it will be necessary to replace Li_xCoO_2 electrode by another one. In this aim, Li_xFePO_4 is a promising cathode material when the electrolyte has a low electrochemical stability because its operating voltage is lower than traditional cathodes such as Li_xCoO_2 or Li_xNiO_2 (3.5 V versus Li) [46].

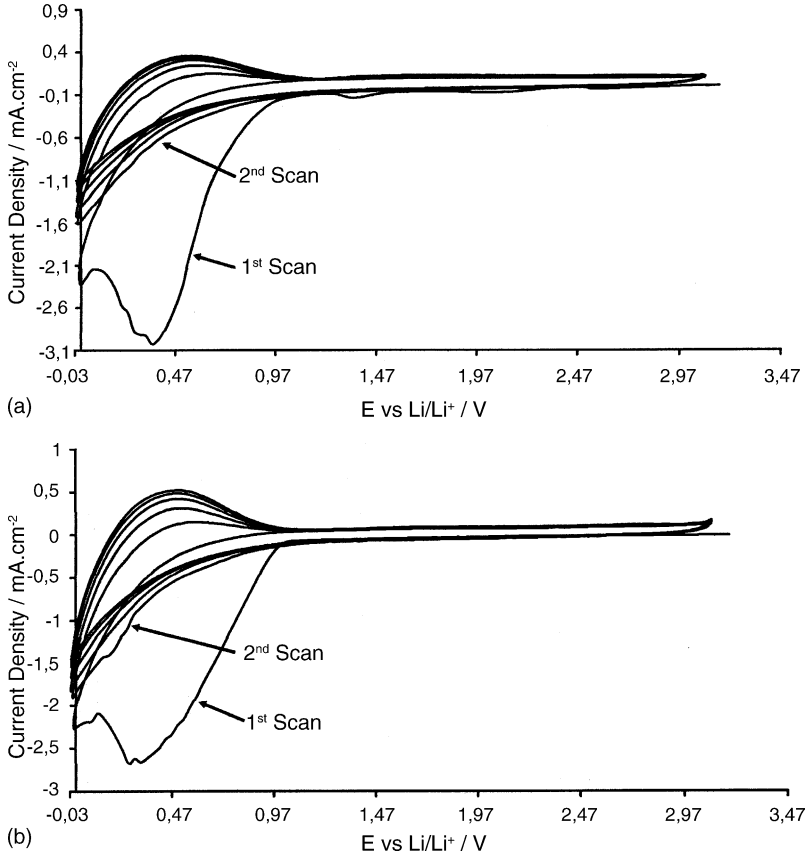

Fig. 8. Cyclic voltammetry at a graphite electrode (scan rate: 0.5 mV s^{-1}) in MeOx:EC x(MeOx) = 0.5 in presence of (a) $LiPF_6$; (b) $LiBF_4$.

3.3.3. Electrochemical behavior at a graphite electrode

Figs. 8 and 9 show successive cyclic voltamogramms at a graphite electrode in a half-cell with MeOx:EC (x(MeOx) = 0.5) and MeOx:DMC (x(MeOx) = 0.4) mixtures in presence of $LiPF_6$ or $LiBF_4$. In MeOx:EC electrolytes (Figs. 8a and b), the reduction of the electrolyte begins at 1 V with a maximum located at 0.3 V (first scan). Lithium insertion occurs till −0.02 V but no deinsertion is observed in the reverse scan. In the next scans, the reduction peak disappears and lithium insertion–deinsertion does not occur with both electrolytes. The large reduction peak at the first scan is attributed to the formation of a passivative film onto the graphite electrode.

In MeOx:DMC electrolytes, at the first scan, the reduction peak attributed to the formation of the passivative layer onto the graphite electrode begins at 0.9 V and the maximum is located at 0.1 V for MeOx:DMC + $LiPF_6$ (Fig. 9a) and 0.3 V for MeOx:DMC + $LiBF_4$ (Fig. 9b). The reduction peak corresponding to the formation of the passivative film for MeOx:DMC + $LiPF_6$ electrolytes exhibit three shoulders which are not observed with the others electrolytes. Solvent co-intercalation and partial destruction of the graphite should also be considered due to the strong intensity of the peak and the poor reversibility of the process. During the successive cyclic voltamogramms, no lithium insertion occurs in presence of $LiPF_6$ whereas partial insertion and deinsertion of lithium occurs in MeOx:DMC + $LiBF_4$ electrolyte. At the second and next scans, a reduction peak begins at 1.3 V with a maximum located at 1.14 V. This peak is not observed when MeOx:EC mixture is used as electrolytes.

As seen in Figs. 8 and 9, film formation occurs near 1 V in all electrolytes. Reduction of the electrolytes is only achieved near 0 V. This means that solvent molecules are able to diffuse through the film to the electrode. As the film is permeable to the solvent, an intercalation of solvent molecules is highly probable leading to partial graphite exfoliation. This explains that, upon the reverse scan, little lithium de-intercalation is obtained. The difference between $LiPF_6$- and $LiBF_4$-based electrolytes may be due to the fact that the film has a lower solvent permeability in the case of $LiBF_4$ as elsewhere reported in γ-butyrolactone based electrolyte [44]. This is confirmed by the galvanostatic test reported in Figs. 10 and 11.

Galvanostatic chronopotentiometries at a graphite electrode in presence of MeOx:DMC + $LiPF_6$ and MeOx:EC + $LiPF_6$ shows that that no significant insertion–deinsertion of lithium occurs in presence or absence of the Celgard separator. For MeOx:EC + $LiBF_4$ electrolyte, partial insertion of lithium is only possible in absence of separator due to the low wettability of the Celgard separator. The same phenomenon was observed using γ-butyrolactone at low temperature when the surface tension of the solvent increases [44]. In Fig. 10 is displayed

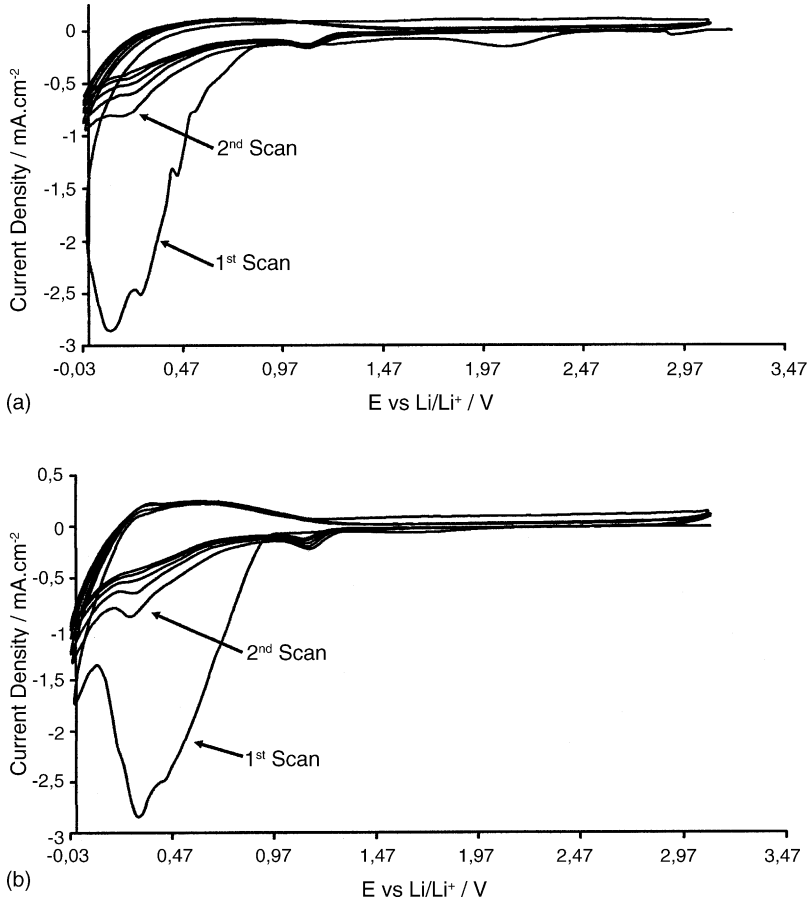

Fig. 9. Cyclic voltammetry at a graphite electrode (scan rate: 0.5 mV s^{-1}) in MeOx:DMC x(MeOx) = 0.4 in presence of (a) $LiPF_6$; (b) $LiBF_4$.

the evolution of the reversible and irreversible capacities during charging–discharging cycles at a graphite electrode for a charge and discharge rate of 15 h per charge or discharge (*C*/15) in absence of separator. In the first cycle, the high value of the irreversible capacity is due to the formation of a passivative layer onto the graphite electrode. In the next cycles, the irreversible capacity decreases significantly but remains close to 25 mAh g^{-1}. After the first cycle, the electrolyte is still reduced to form the passivative layer owing to the low stability of this film which may be partially

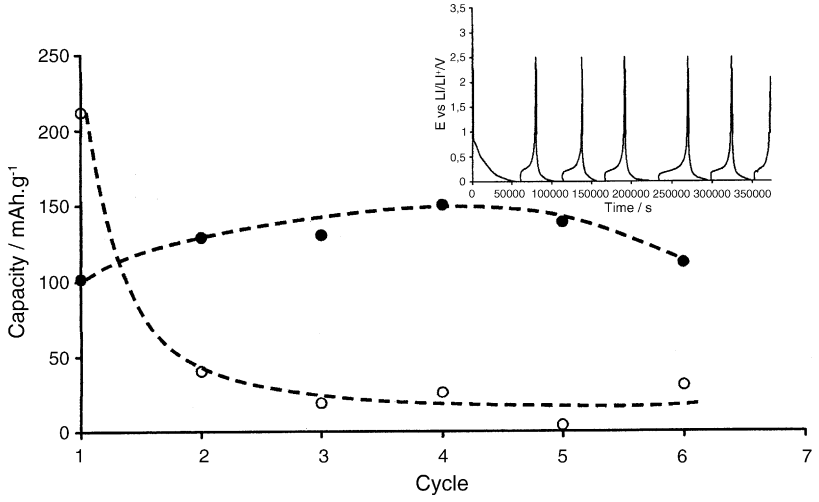

Fig. 10. Reversible C_{rev} (●) and irreversible C_{irr} (◯) capacities during the cycling ability test at a graphite electrode at a rate of *C*/15 (15 h per charge or discharge) in presence of MeOx:EC x(MeOx) = 0.5 + $LiBF_4$ (1 M).

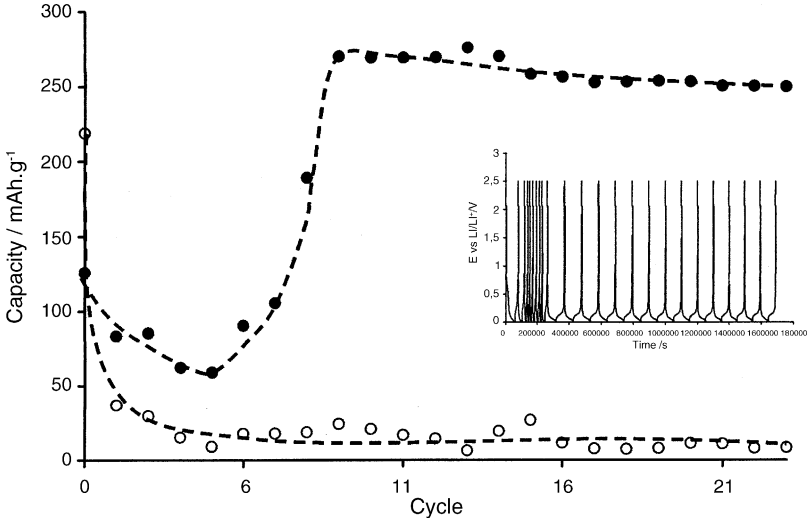

Fig. 11. Reversible C_{rev} (●) and irreversible C_{irr} (○) capacities during the cycling ability test at a graphite electrode at a rate of $C/15$ (15 h per charge or discharge) in presence of MeOx:DMC $x(\text{MeOx}) = 0.4 + \text{LiBF}_4$ (1 M).

dissolved during the discharge. The reversible capacity represents 50 percent of the theoretical capacity of the electrode (280 mAh g^{-1}). The passivative film does not allow an easy insertion and deinsertion of lithium into the electrode. No more than six cycles have been performed because of the formation of dendrites involving short-circuits due to the absence of Celgard separator in the cell. The huge irreversible capacities in the first cycle, the remaining irreversible capacity of 25 mAh g^{-1} in the following cycles and the low reversible capacity show that the electrolyte is strongly reduced and probably the graphite matrix partially destroyed. Hence this solvent is not suitable for graphites.

In order to enhance the wettability of the Celgard separator, DMC has been used with MeOx instead of EC. The cycling ability behavior of MeOx:DMC + LiBF_4 ($x(\text{MeOx}) = 0.4$) electrolyte is reported in Fig. 11. The reversible capacity decreases during the first six cycles and remains lower than the theoretical capacity (280 mAh g^{-1}). After the sixth cycle, the reversible capacity increases and remains close to 280 mAh g^{-1}. The passivative film is fully formed onto the graphite electrode after the fifth cycle as the irreversible capacities remains close to 8 mAh g^{-1}. Nevertheless, nine cycles are necessary to obtain a high quality passivative film by altering the insulator properties and the porosity of the passivation film during lithium insertion–deinsertion. A low loss of reversible capacity (0.4% per cycle) is observed when the passivation film is completely formed on the graphite electrode.

4. Conclusion

Mixtures of 3-methyl-2-oxazolidinone (MeOx) with ethylene carbonate (EC) or dimethyl carbonate (DMC) in presence of lithium salt such as lithium hexafluorophosphate (LiPF_6) or lithium tetrafluoroborate (LiBF_4) have been optimized for their use in lithium batteries. The optimized electrolytes in term of conductivity and viscosity are MeOx:EC, $x(\text{MeOx}) = 0.5$ and MeOx:DMC, $x(\text{MeOx}) = 0.4$ with LiBF_4 or LiPF_6 as lithium salt. The low wettability of the Celgard 2000 membrane by MeOx:EC electrolytes prevents its use in lithium batteries. Only MeOx:DMC + LiBF_4 (1 M) electrolyte wets the separator and permit a cycling ability at a graphite electrode. Nevertheless, a reasonable cycleability of the graphite electrode is reached only after the sixth cycle and the irreversible capacity in the first cycles is huge. Hence, MeOx based electrolytes does not permit a good cycling ability at a graphite electrode.

The low oxidation potential (3.8 V versus Li/Li^+) of the MeOx-based electrolytes at a Li_xCoO_2 electrode does not allow its use as positive electrode in lithium batteries when MeOx:EC or MeOx:DMC in presence of LiBF_4 are used as electrolyte. MeOx seems to be inadequate both for Li_xCoO_2 and graphite. Future works will concern the investigation of others positive electrodes with a lower intercalation–deintercalation potential than Li_xCoO_2 such as Li_xFePO_4 electrode and $\text{Li}_4\text{Ti}_5\text{O}_{12}$ as negative electrode but it will involve an important decrease of the operating voltage of the battery.

References

[1] D. Billaud, F.X. Henry, P. Willmann, Mater. Res. Bull. 28 (1993) 477.
[2] T. Ozhuku, Y. Iwakoshi, R. Sawai, J. Electrochem. Soc. 140 (1993) 2496.
[3] H.L. Huffman, P.G. Sears, J. Sol. Chem. 1 (2) (1972) 187.
[4] A. Webber, J. Electrochem. Soc. 138 (1991) 2586.
[5] M. Wakihara, in: O. Yamamoto (Ed.), Lithium Ion Batteries Fundamentals and Performance, Wiley-VCH, Berlin, 1998.
[6] S.I. Tobishima, T. Okada, Electrochim. Acta 30 (12) (1985) 1715.
[7] M.C. Smart, B.V. Ratnakumar, S. Surampudi, J. Electrochem. Soc. 146 (2) (1999) 486.

[8] G. Pistoia, M. de Rossi, B. Scosati, J. Electrochem. Soc. 117 (1970) 500.
[9] M.D. Jackson, P.G. Sears, J. Chem. Eng. Data 24 (3) (1979) 199.
[10] H.L. Huffman, P.G. Sears, J. Sol. Chem. 1 (2) (1972) 187.
[11] G.G. Botte, R.E. White, Z. Zhang, J. Power Sources 97–98 (2001) 570.
[12] Z. Zhang, D. Fouchard, J.R. Rea, J. Power Sources 70 (1998) 16.
[13] U. von Sacken, E. Nodwell, A. Sundher, J.R. Dahn, Solid State Ionics 69 (1994) 284.
[14] J.R. Dahn, E.W. Fuller, M. Obravae, U. von Sacken, Solid State Ionics 69 (1994) 265.
[15] A. Du Pasquier, F. Disma, T. Bowmer, A.S. Gozdz, G. Amatucci, J.M. Tarascon, J. Electrochem. Soc. 145 (1998) 472.
[16] M.A. Gee, F.C. Laman, J. Electrochem. Soc. 140 (1993) L53.
[17] J.-S. Hong, H. Maleki, S. Al Hallaj, L. Redey, J.R. Selman, J. Electrochem. Soc. 145 (1998) 1489.
[18] M.N. Richard, J.R. Dahn, J. Electrochem. Soc. 146 (1999) 2068.
[19] A. Ohta, H. Koshina, H. Okuno, H. Murai, J. Power Sources 54 (1995) 6.
[20] E.P. Roth, Abstract 388, The Electrochemical Society Meeting Abstracts, vol. 99-2, Honolulu, HI, 17–22 October, 1999.
[21] K. Kumai, H. Miyashiro, Y. Kobayashi, K. Takei, R. Ishikawa, J. Power Sources 81/82 (1999) 715.
[22] Y. Uosaki, T. Hamaguchi, T. Moriyoshi, Fluid Phase Equilibr. 136 (1997) 299.
[23] R. Naejus, D. Lemordant, R. Coudert, J. Chem. Thermodyn. 29 (1997) 1503.
[24] C.G. Barlow, Electrochem. Solid State Lett. 2 (1999) 362.
[25] U. Heider, R. Oesten, M. Jungnitz, J. Power Sources 81 (1999) 119.
[26] K. Tasaki, K. Kanda, S. Nakamura, M. Ue, J. Electrochem. Soc. 150 (2003) A1628.
[27] D. Aurbach, J. Power Sources 89 (2000) 206.
[28] M. Takehara, M. Ue, N. Sato, Y. Sakata, Proceedings of the First Battery Symposium in Japan, Nagoya, November 20–22, 2000.
[29] J. Katzhendler, L.A. Poles, H. Dagan, S. Sarel, J. Chem. Soc. B (1973) 1035.
[30] A. Chagnes, M. Diaw, B. Carré, P. Willmann, D. Lemordant, J. Power Sources 145 (2005) 82–88.
[31] J.F. Kincaid, H. Eyring, A.E. Stearn, Chem. Rev. 28 (1941) 301.
[32] J.-C. Justice, in: B.E. Conway, J.O'M. Bockris, E. Yeager (Eds.), Comprehensive Treatise of Electrochemistry, vol. 5, Plenum Press, New York, 1983, Chapter 3.
[33] D. Brouillette, G. Perron, J. Desnoyers, Electrochem. Acta 44 (1999) 4721.
[34] Y. Aihara, K. Sugimoto, W.S. Ptice, K. Hayamizu, J. Chem. Phys. 113 (2000) 1981–1991.
[35] C. Ghosh, J. Chem. Soc. 113 (1918) 449.
[36] G. Ruff, K. Palinkas, Combos, J. Chem. Soc. Faraday Trans. 2 (77) (1981) 1189.
[37] R.A. Robinson, R.H. Stokes, Electrolyte Solution, 2nd ed., Butterworth, London, 1959, p. 226.
[38] G.W. Murphy, J. Chem. Soc. Faraday Trans. 2 (79) (1983) 1607.
[39] A. Chagnes, B. Carré, D. Lemordant, P. Willmann, Electrochim. Acta 46 (2001) 1783.
[40] A. Chagnes, B. Carré, D. Lemordant, P. Willmann, J. Power Sources 109 (2002) 203.
[41] A. Chagnes, S. Nicolis, B. Carré, P. Willmann, D. Lemordant, ChemPhysChem 4 (2003) 559.
[42] D. Lemordant, B. Montigny, A. Chagnes, M. Caillon-Caravanier, F. Blanchard, G. Bosser, B. Carré, P. Willmann, in: Naoaki Kumagai, Shinichi Komaba (Eds.), "Viscosity–conductivity relationships in concentrated lithium salt organic solvent electrolytes", "Material Chemistry in Lithium Batteries", Research Signpost, 2002, p. 344.
[43] M. Caillon-Caravnier, G. Bosser, B. Claude-Montigny, D. Lemordant, J. Electrochem. Soc. 149 (9) (2002) E340.
[44] A. Chagnes, B. Carré, P. Willmann, R. Dedryere, D. Gonbeau, D. Lemordant, J. Electrochem. Soc. 150 (9) (2003) A1255.
[45] I. Geoffroy, A. Chagnes, B. Carré, D. Lemordant, P. Biensan, S. Herreyre, J. Power Sources 112 (2003) 191.
[46] K. Kriebel, A. Guerfi, J. Shim, M. Armand, M. Gauthier, K. Zhaghib, J. Power Sources 119–121 (2003) 951–954.